学位申請論文

小川哲也

主論文

SAXS from the Surfaces of Polymer Crystals

Small-Angle X-Ray Scattering from the Surfaces of Polymer Crystals

Tetsuya Ogawa

Department of Physics, Faculty of Science, Kyoto University, Sakyo-ku, Kyoto 606

(Received

Synopsis

Surface structure of polyethylene crystals is examined by small-angle X-ray scattering (SAXS) Folded chain crystals crystallized isothermally and extended chain crystals annealed isothermally showed SAXS obeying the Porod's law in a range of scattering vector from $10^{-1.2}$ to $10^{-0.5}$ Å^{-1}; the surfaces of these crystals are smooth above a scale of length of 20 Å. This result suggests that the thickening process of polymer crystals is controlled by nucleation and growth. Fractal surfaces reported previously are related with the fluctuation of driving force for the thickening; the fluctuation has power-law correlation in space or time

KEYWORDS: SAXS, polymer, surface, fractal, polyethylene, Porod's law. Langevin equation, fractional Brownian surface, power-law.

§1. Introduction

Polymers crystallize from the melt or solution in the form of thin lamellae, folded chain crystals (FCC), of a few tens of nanometers thick and several microns wide at ordinary conditions Some polymers like polyethylene (PE) crystallize from the melt at high pressure in the form of thick lamellae, extended chain crystals (ECC), of few microns thick and several tens of microns wide. In these crystals, the polymer chains are almost normal to the lamellae and fold back at the surface. These crystals thicken along the chain direction by annealing at a temperature higher than the crystallization temperature. The mechanisms of crystallization and thickening of these lamellae have attracted much attention in polymer science. Lateral growth of FCC crystallization was basically controlled by the secondary nucleation of the chain stems at the growth faces.[1] ECC was firstly observed for polyethylene annealed at high pressure.[2] The formation of ECC was related with the hexagonal form at high pressure.[3] In this hexagonal form, binding energy between the stems is smaller than in the ordinary orthorombic form since the conformation of a PE chain is in disorder.[4,5] Hence the thickening along the chain direction is easier to give rise to ECC. Recently, these crystallization mechanisms have been reconsidered in detail theoretically or experimentally Hikosaka[6] proposed a unified growth mechanism of the formation of FCC and ECC, assuming a two-dimensional nuleus which grows not only along the direction normal to the chain axis but also along the chain direction by sliding diffusion.

In connection with the thickening mechanism, it is important to examine the surface structure of the lamellar crystals of polymers, especially of ECC which crystallizes in the disordered hexagonal phase.

Small-angle X-ray scattering (SAXS) has been widely used for the investigation of submicroscopic structure (from several to several tens of nanometers) In particular, the scattering in the so-called Porod's region (the region of scattering vector much larger than the inverse of scatterer's size) gives the information on the surface structure of scatterers. The well-known Porod's law[7] is that the scattering intensity, I(q), from materials with smooth surfaces is proportional to q^{-4}, where $q = 4\pi\sin\theta/\lambda$ is the magnitude of the scattering vector, 2θ the scattering angle, and λ the X-ray wave length. Since the fold surfaces of these lamellar crystals are much wider than the lateral surfaces, the SAXS intensity in the Porod's region is predominantly attributed to the scattering from the fold surfaces; the structural information on the fold surface can be obtained.

In a previous paper.[8] it has been shown that the scattering intensity from the ECC of polyethylene or polytetrafluoroethylene (PTFE) obeyed a power-law with a fractional exponent (α) smaller than 4 in Porod's region: $I \sim q^{-\alpha}$ This exponent is expected for surface fractal.[9]

In this paper, new SAXS results for FCC and ECC of polyethylene are reported and discussed together with the previous results[8] in terms of the theories of crystal growth

and fractal concept.

§2. Experimental

Samples used were high density polyethylenes (NBS unfractionated whole polymer, $M_w = 53,070$ $M_w/M_n = 2.9$ and fractionated polymer, $M_w = 32,100$ $M_w/M_n = 1.1$) The polyethylene films 0.5 mm thick were melted in a Mettler hot stage at 155 ˚C for 10 min, cooled to a crystallization temperature and crystallized isothermally to obtain FCC samples: crystallization temperature $T_c = 126.0$ ˚C, crystallization time $t_c = 30$ min (Sample A) and $T_c = 125.0$ ˚C, $t_c = 1$ h (Sample B) for the fractionated PE; $T_c = 123.0$ ˚C, $t_c = 40$ min (Sample C), 10 h (Sample D) or 50 h (Sample E) and $T_c = 125.0$ ˚C, $t_c = 11$ h (Sample F) for the whole polymer Some samples were annealed at a temperature higher than the crystallization temperature. FCC samples were annealed at a pressure of 6.0 kbar by use of a high-pressure DTA (differential thermal analysis) cell[10] to obtain ECC samples. The specimen was heated up to 245.0 ˚C at a rate of 10 ˚C/min and was annealed for 5 min (Sample H), 2 h (Sample I) or 10 h (Sample J) It was confirmed by DTA that the samples were in the hexagonal phase. After annealing, the specimen were quenched to room temperature and pressure was released. It was confirmed that these samples were ECC by the fact that no peaks were found within the accessible q-range in the SAXS profiles; the long periods are larger than 1000 Å. Some FCC samples were annealed in the orthorombic phase (6.0 kbar and 223.0 ˚C: Sample G) just below the phase transition temperature to the hexagonal phase.

SAXS experiment was carried out by a 6-m SAXS camera at HIXLAB of Kyoto University [11] The X-ray is CuKα from a fine-focus X-ray generator (RU-1000C3 of Rigaku Corporation, Japan) operated at 3.5 kW. Isotropic two-dimensional intensity collected by a two-dimensional position-sensitive proportional counter was subtracted by the intensity of background and corrected for the non-uniformity of detector sensitivity and then circularly averaged to give the one-dimensional (1D) data. The sample-to-detector distance employed was either 0.65 or 1.65 m. The two 1D data (higher and lower angle regions) were superposed to get the best fit at the overlapped region of scattering angle The angular region obtained corresponded to Bragg spacing from 10 to 1000 Å.

§3. Results

Figure 1 shows the typical 1D SAXS data, $I_a(q)$, from FCC of the fractionated polyethylene after the correction of background and detector sensitivity There is an increase in intensity at high angles due to the scattering from the amorphous part in the polymer sample and/or by the thermal density fluctuation with long wave length. These contributions, $I_b(q)$, were subtracted by the Ruland's method,[12] in which we assume that

$$I_b(q) = A\exp(Bq^2), \qquad (1)$$

where A and B are constants. Figure 2 is the plot of ln I_a vs q^2 of the data of Fig. 1. The solid line was obtained by the least square fit of the data in the high angles; eq. (1) holds.

The subtracted intensity, I(q), thus obtained is shown in Fig. 3. The same procedures were performed for all the data from the FCC and ECC.

Figure 3 shows the SAXS intensity, I(q), in log-log plot for the FCC of PE (Samples A ~ F). There are peaks corresponding to the periods of stacking lamella. In a range from $10^{-1.2}$ to $10^{-0.5}$ of q, the data points lie on straight lines with a slope ($-\alpha$) of -4.0. which shows the Porod's law; the lamellar surfaces are flat and sharp Since we have obtained the Porod's law for the samples of the unfractionated whole polymer (Sample C ~ F), a broad distribution of chain length does not prevent the FCC crystallized isothermally from having flat and sharp surfaces. It is to be noted that the peak position itself shifted to lower angles for higher crystallization temperature or longer crystallization time; the lamellae thicken with increasing temperature and time.

For the annealed FCC, we have obtained the similar SAXS to that of the FCC crystallized isothermally Figure 4 shows the SAXS intensity, I(q), in log-log plot for the whole polymer crystallized at 123.0 °C for 40 min and successively annealed at 223.0 °C, 6.0 kbar (in the orthorombic phase) for 5 min (Sample G) This figure is similar to Fig. 3. In the Porod's region the exponent α is 4.0 for a range from $10^{-1.0}$ to $10^{-0.5}$ of q.

Figure 5 shows the SAXS intensity from the whole polymer ECC crystallized at 123.0 °C for 40 min and successively annealed in the hexagonal phase (Samples H ~ J) No peaks in SAXS are observed for the ECC in the q-range studied; thickness of lamella

is thicker than 1000 Å. In a range from $10^{-1\ 0}$ to $10^{-0\ 5}$ of q, the Porod's law again holds even for the crystals annealed in the disordered hexagonal phase.

§4. Discussion

In the previous paper.[8] the possibility of fractal surface of polymer crystals was proposed on the basis of the fact that the SAXS intensity I(q) for PE and PTFE obeyed the power-law with the fractional exponents of -3.2 and -3.3 respectively, in a range from $10^{-2\ 0}$ to $10^{-0\ 5}$ of q.

Since Mandelbrot[13] has proposed the fractal concept, fractal nature of the aggregates of colloidal particles have widely been studied in real systems and computer simulations.[14] In particular, for surface fractals, the fractal dimensions have been determined by scattering experiment.[9] :SAXS,[15,16] small-angle neutron[17,18] or light scattering[19] (SANS, SALS)

Fractal is the self-similar structure, which has the invariability on the change of observing scale There are two kinds of fractals.[20] One is self-similar fractal which is invariant for an isotropic change of scale; the other is self-affine fractal which is invariant for an anisotropic change of scale. For example, if the surface is self-affine, the mean square of the difference of height h(**r**) between two points at a distance of r is given by the following equation:

$$\langle [h(\mathbf{r})-h(0)]^2 \rangle \sim r^{2H}, \tag{2a}$$

$$H = d-D, \tag{2b}$$

where d is the space dimension and D is the fractal dimension.

Bale and Schmidt[21] derived the scattering intensity from fractal surfaces in the Porod's region modifying a procedure developed for analysis of the small-angle scattering from materials with smooth boundary surfaces.[22] They calculated the probability Z(r) that if a point lies in a region occupied by material, a second point at a distance of r from the first point also will be in an occupied region. The density correlation function, P(r), is given by

$$P(r) = [Z(r)-c]/[1-c]$$
$$\sim 1-Kr^{3-D}, \quad (r\to 0), \tag{3}$$

where c is a fraction of the occupied region and K is a constant. The exponent 3-D is caused by an assumption that the volume of boundary region is proportional to the number of boxes with edge r needed to cover over the boundary surface of the occupied region; the number is proportional to r^{-D} due to fractal property The scattering intensity is given by the Fourier transform of P(r):

$$I(q)\sim q^{-\alpha}, \quad \alpha = 6-D, \tag{4}$$

in the Porod's region of q.

In this section, firstly the theories on the surface structure of crystals is reviewed, and secondly the previous and present SAXS results are discussed on the basis of the theories.

Relating to surface roughness, roughening transition is to be considered. Roughening transition was first proposed by Burton, Cabrera and Frank (BCF)[23] for the system of two-state Solid-on-Solid (SOS) model. Only two levels of height were allowed for each surface site on a square lattice; the

interaction between the nearest neighbors with different height was taken account of This system was the same class as the two-dimensional Ising model which was rigorously treated by Onsager [24] The order parameter, excess surface energy, increases gradually from zero with increasing temperature, and at the vicinity of the phase transition temperature increases rapidly and then approaches to the maximum value after the transition; the surface is flat below the transition temperature and is rough above it. Several models with many-level state have been studied, taken account of other interactions, with approximate methods or Monte Carlo simulations.[25] It has been clarified that the discreteness of a lattice is important for the existence of roughening transition. Chui and Weeks[26] studied a discrete Gaussian model and proved the existence of roughening transition for the model rigorously In low temperatures, a flat surface (facet) is present on crystal surfaces due to the anisotropy of surface tension; the anisotropy is caused by the discreteness of lattice. As temperature increases, the roughness of the surface is increased; the anisotropy of surface tension decreases to make the surface rough.

The above theory is constructed for equilibrium state. For growing crystals in non-equilibrium, the surface profile is more difficult to be determined. When crystallization temperature is above the roughening transition temperature, the surface is rough even at equilibrium. The growth of a crystal may be the adhesive growth controlled by the diffusion of latent heat for crystallization or of crystallizable units or of impurities to

be excluded. The crystallizable units attach to the growing surface randomly; the growth face is rough wether the driving force for crystallization, such as free energy of melting is strong or weak. When the temperature is below the roughening transition temperature, the surface is flat at equilibrium state. If the driving force for the crystallization is still weak, the crystal can grow through the mechanism of nucleation and growth; the surface can be flat. If the driving force is strong, the surface of the growing crystal may become rough kinetically. In a limit of the strong driving force, the crystallizable units rain down onto a substrate along straight-line trajectories until they reach the surface and become part of a crystal: random deposition model. In that model, the surface height distribution obeys a Poisson process; $D= 3$.

The results that $\alpha= 4$ for the FCC and ECC in the present study show that the fold surfaces of these lamellar crystals are flat. This is consistent with the theory of nucleation theory and growth developed by Lauritzen and Hoffman[1]; in the theory, the fold length is assumed to be the same as that of the initial stem (secondary nucleus) Recently, Keller et al [27] have observed that the lamellar crystal of polyethylene thickens during crystallization. Hikosaka[6] proposed sliding diffusion for the thickening mechanism during crystallization. It may be reasonable that there occurs thickening of lamellar crystals by the annealing during crystallization from the melt, particularly in the hexagonal phase. On the other hand, it is well known that

when polymer crystals are annealed above the crystallization temperature, the thickness of lamellae increases linearly with the logarithm of annealing time except for an initial period of rapid thickening. Hirai and Yamashita[28] proposed the mechanism of nucleation and growth on the fold surface for this logarithmic increase. Sanchez et al.[29] explained this increase in terms of thermodynamics. The driving force for thickening comes from the difference between the surface free energy of the fold surface and that of the lateral surface; the surface free energy of the fold surface is much larger than that of the lateral surface. A thin and wide lamella becomes a thick and narrow lamella, namely more stable one. The segment of a chain is transported to the fold surface by the diffusion of chain slacs or solitons of twisted kinks which are initiated at chain ends by thermal motion, or by sliding diffusion of the stems The result that $\alpha = 4$ for FCC crystallized isothermally and ECC annealed in hexagonal phase can be explained by the model of nucleation and growth described above and these samples were crystallized or annealed below the roughening transition temperature.

The previous SAXS experiment showed that $\alpha = 3.2$ and 3.3 for ECC of PE and PTFE respectively.[8] It is to be noted that α smaller than 4 cannot be deduced from the boundary with a continuous decrease in electron density from crystal region to amorphous region.[30] In that case, the SAXS intensity decreases rather more rapidly with q than q^{-4}: $\alpha > 4$. Accordingly these surfaces may be sharp and rough in spite of the lower

tempetature than the roughening transition. Therefore the driving force for thickening must be very strong and the surface tension stabilizing the fold surface to be flat has to be neglected. The surface tension comes from the free energy of excess lateral surfaces appearing due to rough fold surface. In the hexagonal phase the free energy of lateral surface is small. In the initial period of the high-pressure crystallization, the driving force for the thickening is so strong that thin lamellae crystallized thicken rapidly The above condition for roughening may be hold. The previous ECC samples of PE had crystallization time too short for the thickening process to be the steady state controlled by the nucleation theory; the thickening stopped during the initial period. The driving force for thickening is strong; the surface tension stabilizing force the surface to be flat is weak. Therefore the surfaces become rough. We proposed these as fractally rough surface.[8] Since overhang is to be prohibited in polymer crytals, the rough surface must be self-affine fractal. What is the surface of D of non-integer?

Mandelbrot and Van Ness proposed the fractional Brownian motion, $B_H(t)$, as a model for noise pattern in solid:[31]

$$B_H(t) = \frac{1}{\Gamma(H+1/2)} \int_{-\infty}^{t} (t-s)^{H-1/2} dB(s), \qquad (5)$$

where dB(s) is a Gaussian probability variable with the average of 0 and the variance of 1 defined at point s The function $B_H(t)$ has the property that $\langle [B_H(t)-B_H(0)]^2 \rangle \sim t^{2H}$; the graph of $B_H(t)$ vs t exhibits self-affine fractal of D= d-H (d= 2 in this

case). Mandelbrot took the two-parameter version for the model of earth's surface: fractional Brownian surface.[32] Concrete way of making this surface is as follows Let prepare flat surface of the altitude of 0 ($h(\mathbf{r})=0$, where $\mathbf{r}=(x,y)$) Take lines L_i on x-y plane at an arbitrary position and arbitrary direction, independently For each point $\mathbf{r}$ on x-y plane at a distance of x_i from L_i, define the height increment $\Delta h_i(\mathbf{r})$ as

$$\Delta h_i(\mathbf{r}) = 2^{-1} Q_i x_i^{H-1/2} \mathrm{sgn}, \tag{6}$$

where Q_i is a probability variable with the average $\langle Q_i \rangle$ of 0 and $\langle Q_i Q_j \rangle = \delta_{ij}$ and sgn= ±1 corresponding to whether the point $\mathbf{r}$ is on the left or right hand side of L_i We sum up $\Delta h_i(\mathbf{r})$ and divide by $\nu^{1/2}$, where ν is the average number of lines L_i between two points on x-y plane at a unit distance. The resulting surface $h(\mathbf{r}) = \nu^{-1/2} \Sigma \Delta h_i(\mathbf{r})$ is the fractional Brownian surface. The vertical section is expressed by $B_H(t)$ in eq. (5) and

$$\sigma^2(\mathbf{r}) \equiv \langle [h(\mathbf{r})-h(0)]^2 \rangle \sim r^{2H} \tag{7}$$

The above mechanism is based on the superposition of the cliffs with the shape of $\nu^{-1/2} \Delta h_i(\mathbf{r})$ For the thickening of polymer crystals, it is difficult to generate such process that the uniform increment Δh_i of lamellar thickness along the line L_i In place of eq (6), we accordingly adopt the following form for $\Delta h_i(\mathbf{r})$:

$$\Delta h_i(\mathbf{r}) \sim Q_i' f(\mathbf{r}-\mathbf{r}_i), \quad f(\mathbf{r}) = r^{H-1/2}, \tag{8}$$

where Q_i' is the probability variable of

$$\langle Q_i' Q_j' \rangle = \delta_{ij} \tag{9}$$

defined at arbitrary position $\mathbf{r}_i$ Summimg up $\Delta h_i(\mathbf{r})$, the

resulting surface is given by the following equation:

$$h(\mathbf{r}) = \sum_{i=1} \Delta h_i(\mathbf{r})$$

$$= \sum_{i=1} |\mathbf{r}-\mathbf{r}_i|^{H-1/2} Q_i' \qquad (10)$$

The variance $\sigma^2(\Delta\mathbf{r})$ is

$$\sigma^2(\Delta\mathbf{r}) = \langle[h(\mathbf{r}+\Delta\mathbf{r})-h(\mathbf{r})]^2\rangle$$

$$= \sum_{i,j} \langle[f(\mathbf{r}+\Delta\mathbf{r}-\mathbf{r}_i)-f(\mathbf{r}-\mathbf{r}_i)] \times[f(\mathbf{r}+\Delta\mathbf{r}-\mathbf{r}_j)-f(\mathbf{r}-\mathbf{r}_j)]\rangle\langle Q_i' Q_j'\rangle$$

$$= \sum_i \langle[f(\mathbf{r}+\Delta\mathbf{r}-\mathbf{r}_i)-f(\mathbf{r}-\mathbf{r}_i)]^2\rangle$$

$$= n\int[f(\mathbf{r}+\Delta\mathbf{r})-f(\mathbf{r})]^2 d\mathbf{r}, \qquad (11)$$

where n is the number density of point $\mathbf{r}_i$ and we have used eq. (9) Substituting eq. (8) into eq (11), we obtain

$$\sigma^2(\Delta\mathbf{r}) = n\int[|\mathbf{r}+\Delta\mathbf{r}|^{H\ 1/2}-r^{H\ 1/2}]^2 d\mathbf{r}$$

$$= n(\Delta r)^{2H}\int[|\mathbf{r}'+\Delta\mathbf{r}/\Delta r|^{H-1/2}-r'^{H-1/2}]^2 d\mathbf{r}',$$

where $\mathbf{r}' = \mathbf{r}/\Delta r$ is used. Since $\Delta\mathbf{r}/\Delta r$ is a unit vector, the integral does not depend on Δr Therefore,

$$\sigma^2(\Delta\mathbf{r}) \sim (\Delta r)^{2H} \qquad (12)$$

This procedure constructing fractal surface is based on the superposition of the independent mountain (or "hollow") described by eq. (8); the mountain is located at an arbitrary position on the surface.

On the other hand, the self-affine fractal surface is interested in the studies of aggregation or vapor deposition on substrate. Several authors have examined the scaling

properties of the surface height and width in a simple model like the Eden model or a ballistic-deposition model by computer simulation or theoretically.[33,34] Edwards and Wilkinson studied another model for rough surface; in the model, granular particles rain down onto the surface and diffuse on the surface to the position of lower height with a short diffusion length.[35] They wrote down the following Langevin equation for the development of the surface profile:

$$\frac{\partial h(\mathbf{r},t)}{\partial t} = M\nabla^2 h(\mathbf{r},t)+\xi(\mathbf{r},t), \tag{13}$$

where $\mathbf{r}$ is (x,y), the first term of the right hand side represents the surface relaxation due to the surface diffusion, and the second term $\xi(\mathbf{r},t)$ is a random-noise term ($<\xi(\mathbf{r},t)\xi(0.0)> \sim\delta(\mathbf{r})\delta(t)$) They showed $\sigma^2(\mathbf{r})= <[h(\mathbf{r},t)-h(0.0)]^2> \sim \ln r$; $D= 3$ for $d= 3$ In the system of $d= 3$, if random-noise term ξ is made by the following superposition of the Gaussian fluctuation,

$$\xi(\mathbf{r},t)= \iint K(\mathbf{r}-\mathbf{r}',t-t')R(\mathbf{r}',t')d\mathbf{r}'dt', \tag{14}$$

where $K(\mathbf{r},t)\sim|\mathbf{r}|^{\rho-2}|t|^{\theta-1}$ and $R(\mathbf{r},t)$ is Gaussian random-noise, ξ has correlation in space and time; $<\xi(\mathbf{r},t)\xi(0,0)>\sim r^{2\rho-2}t^{2\theta-1}$ If the scaling form of $r^{2\chi}g(t/r^z)$ is assumed for $<[h(\mathbf{r},t)-h(0.0)]^2>$, the scaling exponent $\alpha(= 3+\chi)$ is expected to be a fractional value of $3+\rho+2\theta$ ($D= 3-\rho-2\theta$) in order to make eq (13) scale invariant.[36]

In both fractional Brownian surface and Langevin equation, the essential nature lies in the fluctuation force; the force is made by the superposition of the random-noise dB (in eq. (5)) or

R (in eq (14)) with the weight of a power-law with an fractional exponent and has no characteristic length accordingly The origin of the power law in the correlation of fluctuation is not clear The extra field caused by the impurity or defect in crystals may relate to the power law correlation.

Acknowledgements

The author expresses his sincere thanks to Prof Miyaji for helpful discussion and to the committee of HIXLAB of Kyoto University for the use of 6-m SAXS system.

References

1) J I. Lauritzen and J D. Hoffman: J Res. Natl. Bur Stand. **64A** (1960) 73.

2) F R. Anderson: J Appl Phys. **35** (1964) 64.

3) D. C. Bassett: Polymer **17** (1976) 460.

4) T Yamamoto: J Macromol. Sci B **16** (1979) 487

5) D. C. Bassett: Principles of Polymer Morphology (Cambridge University Press, Cambridge, 1981) Chap. 7.

6) M. Hikosaka: Polymer **28** (1987) 1257

7) G. Porod: Kolloid Z. **124** (1951) 83.

8) T Ogawa, S Miyashita, H. Miyaji, S Suehiro and H. hayashi: J Chem. Phys. **90** (1989) 2063.

9) J E. Martin and A. J Hurd: J Appl. Cryst. **20** (1987) 61.

10) T Asahi, Y Miyamoto, H. Miyaji and K. Asai: Polymer **23** (1982) 773.

11) H. Hayashi, F Hamada, S. Suehiro, N. Masaki, T Ogawa and H. Miyaji: J Appl. Cryst **21** (1988) 330.

12) W Ruland: Pure Appl. Chem. **49** (1977) 505

13) B. B. Mandelbrot: The Fractal Geometry of Nature (Freeman, San Francisco, 1982)

14) Fractals in Physics (North-Holland, Amsterdam, Oxford, New York and Tokyo, 1986) ed. L. Pietronero and E. Tosatti

15) A. Höhr H.-B. Neumann, P W. Schmidt, P Pfeifer and D Avnir : Phys. Rev B **38** (1988) 1462.

16) K. D. Keefer and D. W Schaefer: Phys. Rev Lett. **56** (1988) 2376.

17) A. J Hurd, D. W Schaefer and J E. Martin: Phys Rev A **35**

(1987) 2361.

18) R. Vacher, T Woignier and J. Pelous: Phys. Rev B **37** (1988) 6500.

19) J E. Martin and K. D Keefer: Phys. Rev A **34** (1986) 4988.

20) J Feder: Fractals (Plenum Press, New York and London, 1988)

21) H. D. Bale and P. W Schmidt: Phys. Rev Lett. **53** (1984) 596.

22) A. Guinier and G. Fournet: Small-Angle Scattering of X-Rays (Wiley, New York, 1955)

23) W. K. Burton, N. Cabrera and F C. Frank: Philos. Trans R. Soc London A **243** (1951) 299.

24) L. Onsager: Phys. Rev **65** (1944) 117

25) H. Müller-Krumbhaar: Monte Carlo Methods in Statistical Physics (Springer-Verlag, Berlin and New York, 1978) ed. K. Binder Chap. 7

26) S. T Chui and J D. Weeks: Phys Rev B **14** (1976) 4978.

27) J Martinez-Salazar, P J Barham and A. Keller: J Mater Sci **20** (1985) 1616.

28) N Hirai and Y Yamashita: Kobunshikagaku/Chem. (High Polymer Janan) **21** (1964) 173 [in Japanese]

29) I. C. Sanchez, J P Colson and R. K. Eby: J Appl Phys. **44** (1973) 4332.

30) C. G. Vonk: J Appl Crystallogr **6** (1973) 81.

31) B. B. Mandelbrot and J W Van Ness: SIAM Review **10** (1968) 422.

32) B. B. Mandelbrot: Proc. Nat. Acad. Sci. USA **72** (1975) 3825.

33) F Family and T Vicsek: J Phys. A: Math. Gen. **18** (1985)

L75.

34) R. Jullien and R. Botet: J Phys. A: Math. Gen. **18** (1985) 2279.

35) S. F Edwards, F R. S. and D. R. Wilkinson: Proc. R. Soc. Lond. A **381** (1982) 17

36) E. Medina, T Hwa, M. Kardar and Y -C. Zhang: Phys. Rev A **39** (1989) 3053.

Figure captions

Figure 1.

SAXS intensity, $I_a(q)$, for FCC of PE crystallized isothermally. Sample-to-detector distance of 1.65 m was employed for a range from $10^{-2\ 2}$ Å^{-1} to $10^{-0\ 82}$ Å^{-1} of q and 0.65 m for a range from $10^{-1\ 15}$ Å^{-1} to $10^{-0\ 2}$ Å^{-1}

Figure 2.

Log I_a vs. q^2 plot of the SAXS intensity for FCC of PE. The solid line represents $I_b(q)$ subtracted to get I(q)

Figure 3.

Log-Log plot of the SAXS intensity for FCC of PE. The slope of the solid line is -4.0. A: fractionated PE, T_c=126.0 ˚C, t_c=30 min. B: T_c=125.0 ˚C, t_c=1 h. C: unfractionated PE, T_c=123.0 ˚C, t_c=40 min. D: t_c=10 h. E: t_c=50 h. F: T_c=125 0 ˚C, t_c=11 h.

Figure 4

Log-Log plot of the SAXS intensity for FCC of PE annealed in the orthorombic phase at high pressure (Sample G)

Figure 5

Log-Log plot of the SAXS intensity for ECC of PE annealed in the hexagonal phase at high pressure. H: T_a=245 0 ˚C, t_a=5 min, P_a=6.0 kbar. I: t_a=2 h. J: t_a=10 h.

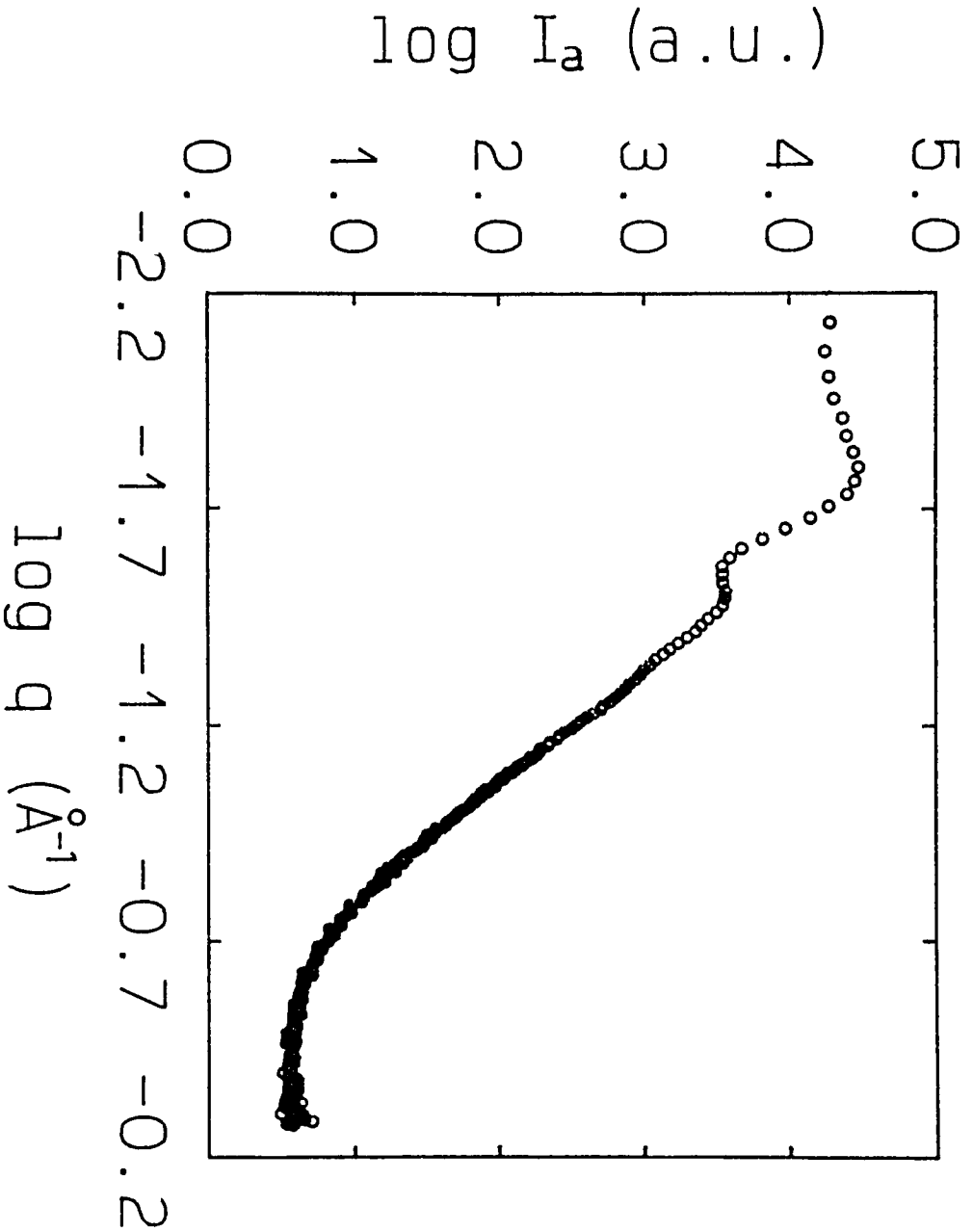

Fig 1

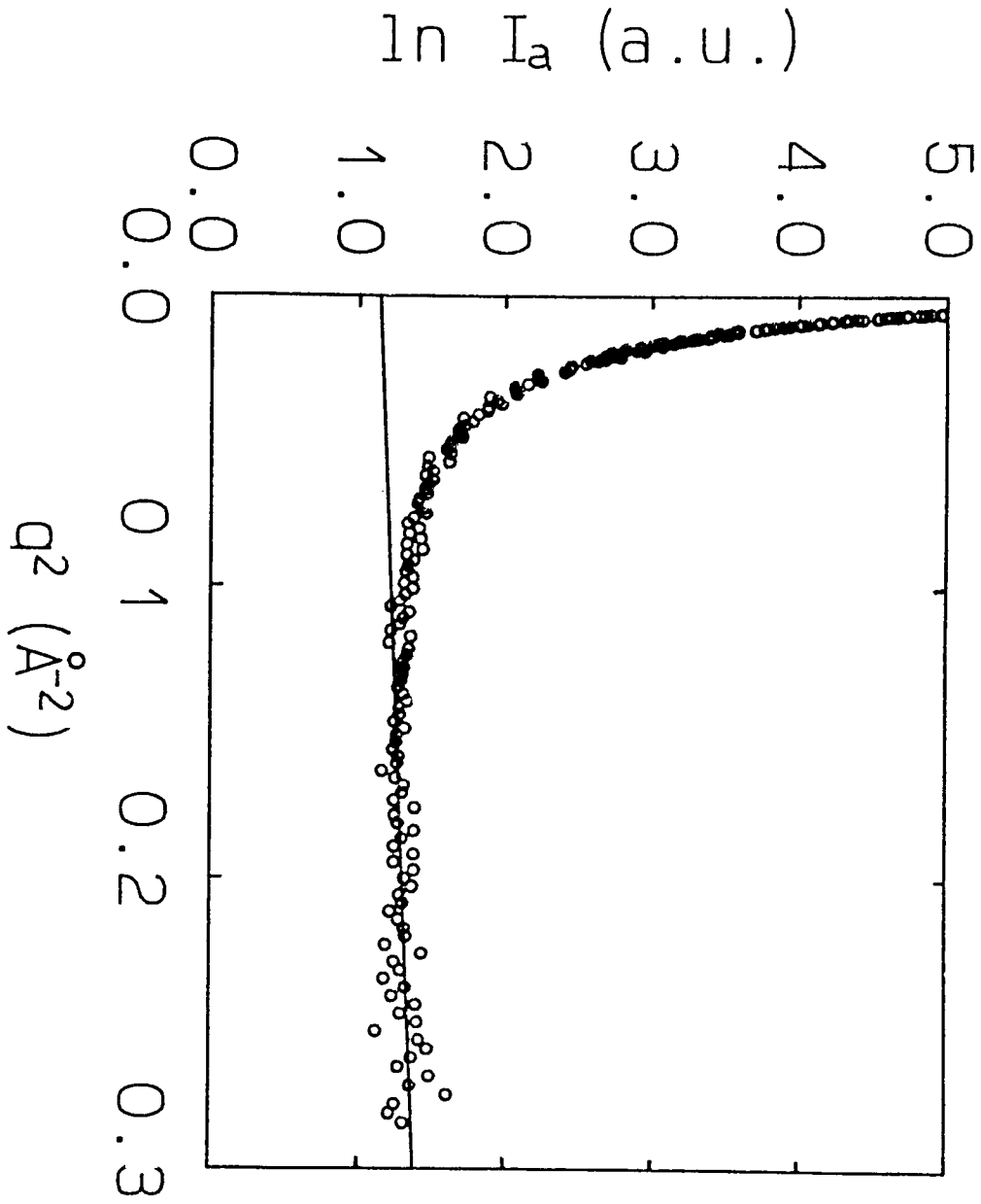

Fig. 2

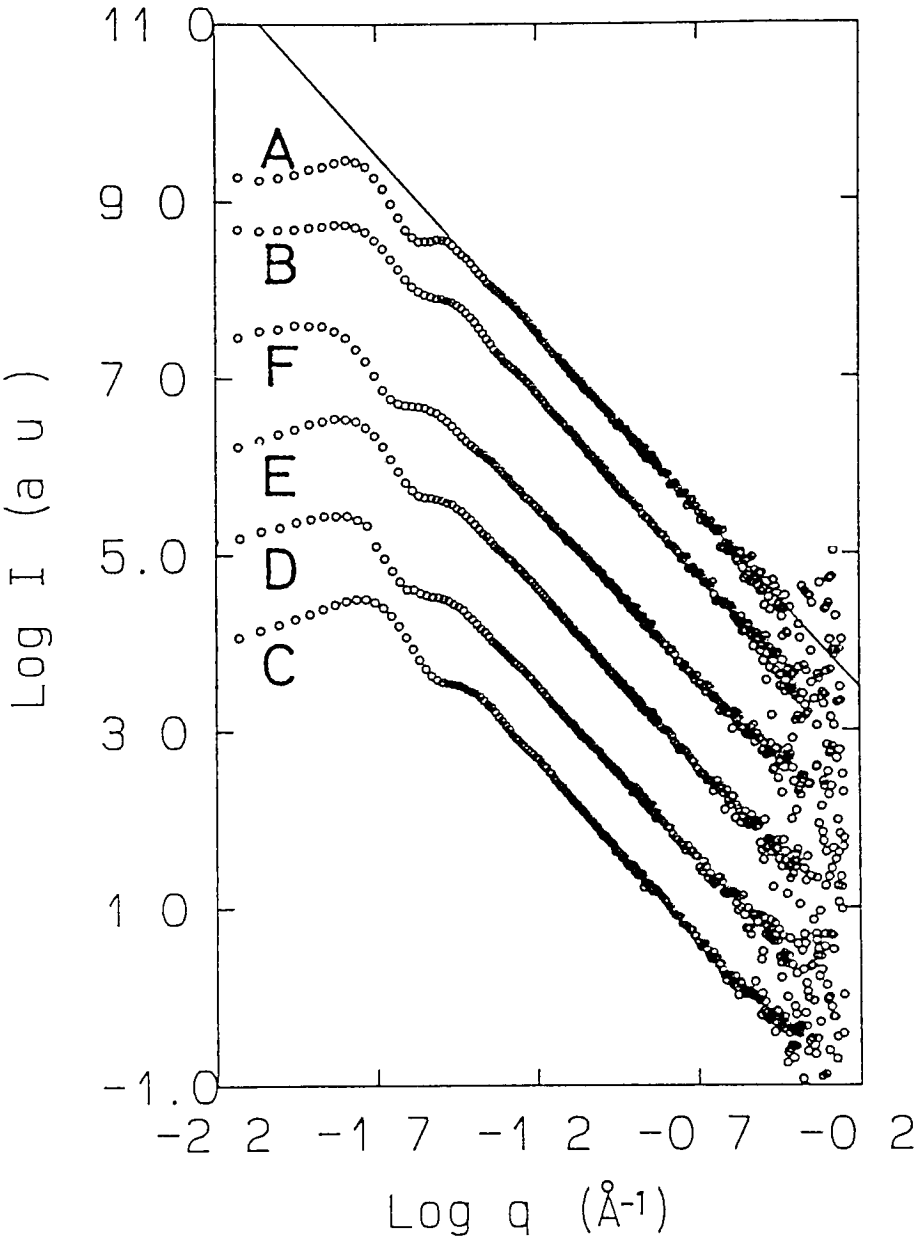

Fig 3

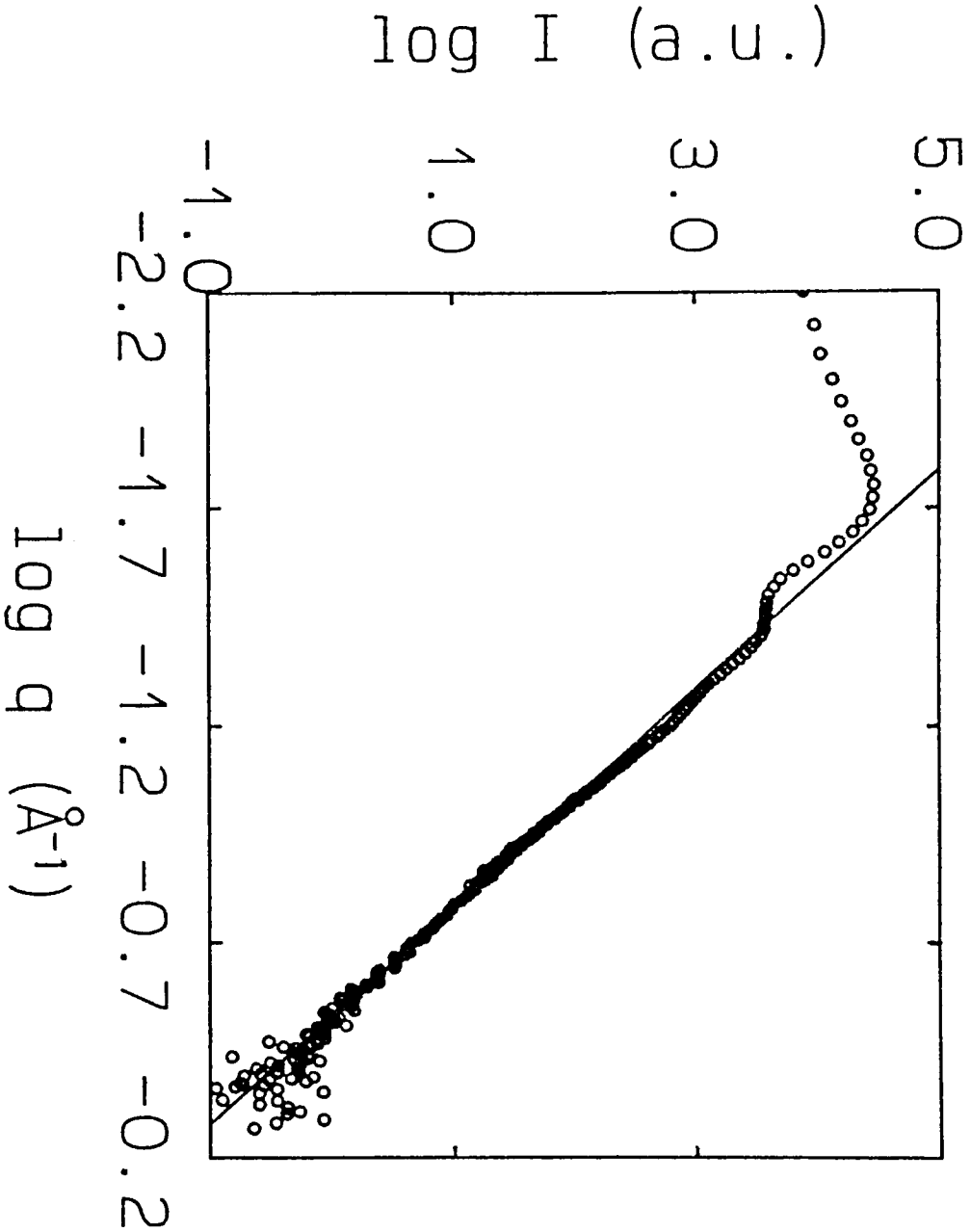

Fig. 4

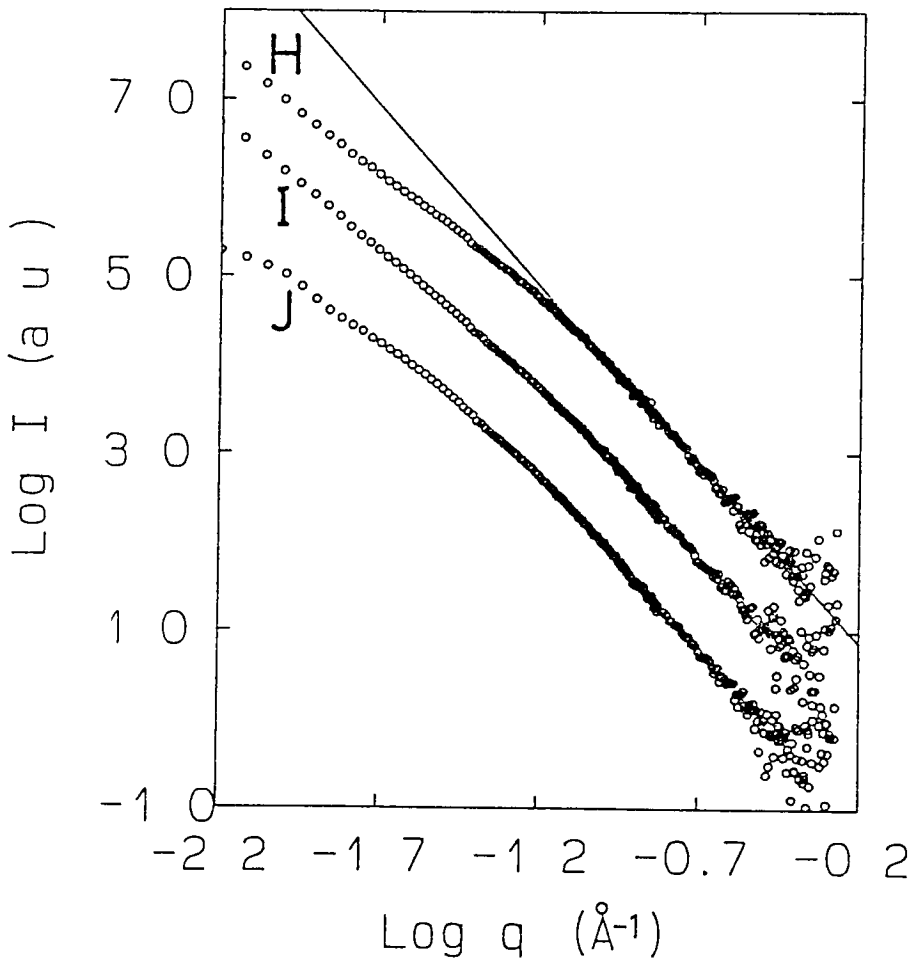

Fig.5